



Cardiac developmental toxicity and transcriptome analyses of zebrafish (*Danio rerio*) embryos exposed to Mancozeb

Yongfeng Wang, Zhiqian Yu, Zunpan Fan, Yiwei Fang, Liting He, Meili Peng, Yuanyao Chen, Zhiyong Hu, Kai Zhao, Huiping Zhang*, Chunyan Liu

Institute of Reproductive Health, Tongji Medical College, Huazhong University of Science and Technology, Hubei 430030, PR China



ARTICLE INFO

Edited by: Dr Yong Liang

Keywords:

Mancozeb
Cardiotoxicity
Zebrafish embryos
Apoptosis
Notch signaling pathway

ABSTRACT

Mancozeb (MZ), an antibacterial pesticide, has been linked to reproductive toxicity, neurotoxicity, and endocrine disruption. However, whether MZ has cardiotoxicity is unclear. In this study, the cardiotoxic effects of exposure to environment-related MZ concentrations ranging from 1.88 μM to 7.52 μM were evaluated at the larval stage of zebrafish. Transcriptome sequencing predicted the mechanism of MZ-induced cardiac developmental toxicity in zebrafish by enrichment analysis of Kyoto Encyclopedia of Genes and Genomes (KEGG) and Gene Ontology (GO). Consistent with morphological changes, the *osm*, *pfkfb3*, *foxf1*, *stc1*, and *mrarp* genes may effect normal development of zebrafish heart by activating NOTCH signaling pathways, resulting in pericardial edema, myocardial fibrosis, and congestion in the heart area. Moreover, differential gene expression analysis indicated that cyp-related genes (*cyp1c2* and *cyp3c3*) were significantly upregulated after MZ treatment, which may be related to apoptosis of myocardial cells. These results were verified by real-time quantitative RT-qPCR and acridine orange staining. Our findings suggest that MZ-mediated cardiotoxic development of zebrafish larvae may be related to the activation of Notch and apoptosis-related signaling pathways.

1. INTRODUCTION

The heart is the first functional organ during fetal development (Moore-Morris et al., 2018). Cell fate decisions at the origin of all cardiac cell lineages are influenced by both genes and the environment; thus, genetic variants or environmental exposures may lead to abnormal heart development (Stadler and Allis, 2012). Congenital heart defects (CHDs) are one of the most common congenital malformations that account for about a third of all birth defects (Kim et al., 2017). CHDs are the leading cause of spontaneous abortions, stillbirths, newborn, and infant deaths, as well as the root cause of various medical abortions (Kim et al., 2017). The detection rate of heart diseases in live births is about 1% (Patel et al., 2021). Both premature and full-term babies with heart defects

have high mortality rates (Tanner et al., 2015). Children who are lucky enough to survive may require medical treatment for the rest of their lives. Approximately 30% of the causes of heart defects are known, whereas the remaining 70% are unknown (Jenkins et al., 2007). CHDs among newborns are closely related to exposure to various compounds during pregnancy, including pesticides, environmental endocrine pollutants, solvents, toxic metals, and other persistent organic pollutants (Salamanca-Fernández et al., 2020). Therefore, the cardiac developmental toxicity of various environmental pollutants must be evaluated to reveal the high-risk factors of CHDs.

Mancozeb (MZ), a class of ethylene disthiocarbamate fungicides, is widely used in various industry and agriculture because of its high efficiency, low cost, and broad spectrum of bactericidal properties,

Abbreviations: MZ, Mancozeb; KEGG, Kyoto Encyclopedia of Genes and Genomes; CHDs, Congenital heart defects; RNA-Seq, transcriptome sequencing; DEGs, differentially expressed genes; DMSO, dimethyl sulfoxide; hpf, hour post fertilization; RTq-PCR, Real-time fluorescence quantitative PCR; AO, acridine orange; ODA staining, o-Dianisidine staining; GO, Gene Ontology; Notch1–4, four Notch receptors; AL, amyloidosis; LC, Immunoglobulin light chain; DLL4, delta-like4; TNF- α ; tumor necrosis factor- α ; TRAIL, TNF-associated apoptosis-inducing ligand; AHRs, aromatic hydrocarbons; AhR, aryl hydrocarbon receptor; HSPs, heat shock proteins; NICD, Notch intracellular domain.

* Correspondence to: Institute of Reproductive Health, Tongji Medical College, Huazhong University of Science and Technology, No.13, Hangkong Road, Wuhan, Hubei, PR China.

E-mail addresses: wfly@hust.edu.cn (Y. Wang), 1625965131@qq.com (Z. Yu), zunpanfan@hust.edu.cn (Z. Fan), evayfang@163.com (Y. Fang), litinhe@hust.edu.cn (L. He), pml@hust.edu.cn (M. Peng), m202075746@hust.edu.cn (Y. Chen), d201781264@hust.edu.cn (Z. Hu), kai_zhao@vip.163.com (K. Zhao), zhpmmed@126.com (H. Zhang), lchy2019@hust.edu.cn (C. Liu).

<https://doi.org/10.1016/j.ecoenv.2021.112798>

Received 23 July 2021; Received in revised form 12 September 2021; Accepted 15 September 2021

Available online 27 September 2021

0147-6513/© 2021 The Author(s). Published by Elsevier Inc. This is an open access article under the CC BY-NC-ND license

(<http://creativecommons.org/licenses/by-nc-nd/4.0/>).

especially in crops (e.g., potatoes, bananas, tomatoes, and oranges), as fungicides (Runkle et al., 2017; Gullino et al., 2010; Hwang et al., 2001). Thus far, MZ have been demonstrated to kill over 400 plant pathogens, and its use continues to expand. In 2014, the global usage of MZ accounted for 20% of pesticide usage (Casida, 2017). High doses of MZ metabolites ranging from ng/L to mg/L levels are often detected in the soil and surrounding water (Bianchi et al., 2020).

The general population is exposed to MZ through the consumption of agricultural products and water contaminated with this fungicide (Mora et al., 2018). In the workplace, workers who produce and are responsible for spraying are exposed to MZ. They inhale this compound through the skin, respiratory tract, or through their digestive tract if they failed to wash their hands after work (Van Wendel De Joode et al., 2014). A cohort study in Costa Rica showed that the median concentration of MZ metabolites in the urine of pregnant women living near banana plantations sprayed with MZ was over five times higher than that of other people in the general population, and 72% of the women's estimated daily intake exceeded the established reference doses (Van Wendel De Joode et al., 2016; Nascimento et al., 2016; Palzes et al., 2019; Rahman et al., 2017). Nevertheless, MZ is rapidly metabolized in humans and poses a low acute toxicity to animals. Nevertheless, previous studies confirmed that exposure to MZ can cause various health hazards, including potential reproductive toxicity, neurotoxicity, endocrine disruption (Asparch et al., 2020). Furthermore, MZ has been recently found to have estrogenic activity (Wang et al., 2021). Exposure during pregnancy will also affect fetal neurodevelopment, such as increasing the risk of autism, hyperactivity disorder, and depression (Nordby et al., 2005). A study evaluated the effects of MZ exposure on rats and rabbits within the concentration limit set by the US Environmental Protection Agency. Results showed that MZ exposure increased maternal mortality, induced spontaneous abortion, led to the development of thyroid disease, and caused other detrimental effect on health (Stephenson and Trombetta, 2020). Conversely, the issue of whether MZ exposure can lead to fetal cardiac dysplasia is unclear. Thus far, only one animal experimental study has shown that MZ can lead to striated muscle fibrosis in rats (Stephenson and Trombetta, 2020). Another toxicological experiment using zebrafish as the biological model also found that MZ exposure can lead to pericardial edema in zebrafish (Paganotto Leandro et al., 2021). Alternatively, the mechanism of MZ-induced myocardial developmental toxicity has not been elucidated yet.

In this study, we evaluated the cardiotoxic effects of MZ on zebrafish, a vertebrate model that has been widely used in recent years in research on developmental genetics and functional genomics (Genge et al., 2016). Zebrafish hearts are increasingly being used as models for studying human heart functions partly because they are similar to humans in terms of heart rate, action potential duration, and morphology (Martin and Waxman, 2021). Moreover, imaging of zebrafish heart can provide whole-heart high-resolution images that can be used in monitoring heart development. Using these images, the process of heart development can be clearly observed. As such, it is known as "the research window of heart development" (Sarmah and Marrs, 2016).

To understand the cardiotoxicity of environmentally relevant concentrations of MZ to zebrafish, we integrated morphological and transcriptional effects to clarify the underlying mechanisms regulating the expression of MZ-induced transcripts. Through morphological measurements, we compared the phenotypes of zebrafish's heart development under different exposure concentrations. We then recorded various abnormalities and proportions in zebrafish heart. To reveal further the various molecular mechanisms of interactions that change during MZ exposure, we performed transcriptome sequencing (RNA-Seq) of zebrafish larvae to quantify the expression of transcripts with high sensitivity and wide genome coverage following MZ treatment (Liu and Wen, 2002). The combination of morphological measurements and transcriptome analysis provides new insights into the mechanism of MZ-induced toxicity to zebrafish larval heart developmental. To the best

of our knowledge, this study was the first to adopt transcriptome methods to study the mechanism of MZ-induced cardiotoxicity in zebrafish. By linking differentially expressed genes (DEGs) with toxicity endpoints, this study identified potential phenotype-specific biomarkers and provided a basis for environmental health risk assessment of MZ.

2. Materials and methods

2.1. Chemical reagents

Mancozeb (MZ, CAS:8018-01-7, 99.7%) and dimethyl sulfoxide (DMSO, CAS:67-68-5, 99.7%) were acquired from Sigma-Aldrich (St. Louis, USA). MZ was dissolved in 5/100,000 DMSO reagent and stored in a refrigerator at 4 °C for later use.

2.2. Zebrafish maintenance and exposure protocols

Wild-type zebrafish (AB line, *Danio rerio*) was maintained in the Model Organism Zebrafish Experimental Platform of the Institute of Reproductive Health, Tongji Medical College, Huazhong University of Science and Technology. The zebrafish were maintained in a circulatory system with dechlorinated tap water (pH 7.0–7.5) at a constant temperature of 28 ± 0.5 °C and 14 h/10 h light/dark cycle. The preservation and collection of zebrafish embryos were performed following the methods described in a previous study (Huang et al., 2018). Fertilized eggs were collected and raised at 28 °C in an incubator. The larvae were anaesthetized with 0.168 mg/mL Tricaine (Sigma-Aldrich) before use (Matthews et al., 2002).

The exposure concentration of MZ (1.88, 2.81, 3.76, and 7.52 μM) was similar to that reported in previous studies (Tilton et al., 2006; Costa-Silva et al., 2018) or a solvent control (0.005% DMSO) (Qiu et al., 2020). Exposure time ranged from 4 hpf to 96 hpf, and zebrafish development was observed. Each dish had 50 embryos. The volume of the exposed system was 3 mL, and each concentration was set to three replicates. Stable MZ concentration was maintained during exposure by changing the fluid at 08:00 and 22:00 every day. Larvae exposed to 96 hpf were selected for the preparation of transcriptome sequencing samples. Sequencing concentration was based on the dose-dependent response curve of zebrafish heart malformations calculated at 96 hpf. The exposure concentration corresponding to the highest slope was selected as the sequencing exposure concentration (3.0 μM) (Ji et al., 2019). Each treatment was run in triplicate (treatment with 3.0 μM MZ and control group with 0.005% DMSO).

2.3. RNA isolation, cDNA library construction, and sequencing

From each sample pool, about 200 larvae were collected, washed with PBS, and quickly frozen in liquid nitrogen for 2 h. The frozen larvae were transferred to a –80 °C refrigerator for subsequent transcriptome sequencing experiment. Zebrafish RNA was extracted via the guanidine isothiocyanate/phenol method (TRIZOL) and purified by the silica gel column of HiPure Universal RNA Mini Kit (R4130-02, MEG). RNA purity was measured using a nanophotometer (Implen, CA, USA). RNA concentration was measured using a Qubit®3.0 fluorimeter (Life Technologies, CA, USA). RNA integrity was assessed using a 2100 RNA Nano 6000 Assay Kit (Agilent Technologies, CA, USA). After the samples passed the test, 3 μg total RNA was taken from each sample as the starting material to construct the transcriptome sequencing library. A library was built using a different index tag by using a NebNext® Ultra™ RNA Library Prep Kit for Illumina® (#E7530L, NEB). For qualified total RNA samples, magnetic beads with Oligo (dT) were used to enrich eukaryotic mRNA. mRNA was broken into short fragments after a fragmentation buffer was added. mRNA was used as a template, and cDNA was synthesized with random hexamers. Buffer solution, DNTPs, RNase H, and DNA Polymerase I were then added to synthesize two-strand cDNA. Double-strand cDNA was purified using AMPure XP

Beads and QIAQuickPCR kits. After the library construction was completed, the library was preliminarily quantified using Qubit3.0, and the library was diluted to 1 ng/ μ L. The INSERT SIZE of the library was tested using Agilent 2100. Real-time fluorescence quantitative PCR (RTq-PCR) was performed using Bio-Rad CFX 96 fluorescence quantitative PCR instrument and Bio-Rad Kit IQ SYBR GRN. The effective concentration of the library was accurately quantified (the effective concentration of the library was > 10 nM) to ensure the quality of the library. Clusters were generated on CBOT by using HiSeq PE Cluster Kit V4-CBOT-HS (Illumina) reagent. The double-ended sequencing (PE) procedure was then run on the Hiseq sequencing platform, and 150 bp double-ended reads were obtained.

2.4. Transcriptomic sequencing

A total of 43.95 Gb of clean data were obtained, and the clean data of all samples reached 7.02 Gb or above. The percentage of Q30 base was 93.82% or above. Clean reads of each sample were sequenced with the designated reference genome, and the alignment efficiency ranged from 90.77% to 92.00%. The expression levels of DEGs in different samples were measured, functionally annotated, and enriched. Appropriate DEGs were selected and analyzed in accordance with the actual situation (edgeR) (Robinson et al., 2010; Afouda et al., 2020), DEseq (Anders and Huber, 2010), and EBseq (Nueda et al., 2018). For the DEG analysis of the samples with biological duplication, differential screening was performed using the Edger software, with fold change ≥ 2 and $p < 0.05$ as the screening criteria. Fold change represents the ratio of expression levels between two samples (groups), and $p < 0.05$ indicated the significance of differential expression.

2.5. RT-qPCR

The results of RNA-Seq were verified via RT-qPCR. Eight different genes, seven of which were upregulated and one was downregulated, related to zebrafish heart development were selected according to the function and expression level of transcriptome genes. The same method for extracting RNA from zebrafish larvae was used to verify the results of transcriptome sequencing. Relative mRNA expression levels were normalized via the $2^{\Delta\Delta CT}$ method and β -actin as the housekeeping gene. Three separate samples were tested three times. The sequences of the primers used in this study are given in Table S1.

2.6. Morphological characteristics

Zebrafish embryos from each exposure concentration were imaged at 96 hpf under a stereomicroscope. Zebrafish pericardial cavity was measured using Image J software (Version 1.49, National Institutes of Health). At least 15 individual embryos were imaged for each concentration at each time point (Y. Li et al., 2020; M. Li et al., 2020). Heart malformation rate and heart rate of zebrafish larvae after 96 h exposure were recorded. Heart rate, defined as heartbeats per minute, was recorded at 96 hpf under a stereomicroscope.

2.7. Tissue sectioning and hematoxylin–eosin staining

At 96 hpf, 10 zebrafish larvae were randomly selected from each exposure concentration group and fixed overnight with 4% paraformaldehyde at 4 °C. After fixation, the larvae were dehydrated by ethanol gradient, transferred to 100% xylene, and then permeated with paraffin wax. Five to eight sections were taken from each group, including the anterior heart region of the yolk sac. Sections routinely stained with hematoxylin and eosin were observed under a microscope (Ming Mei Shot) and photographed.

2.8. o-Dianisidine staining

Several zebrafish larvae in the DMSO and MZ groups exposed to 96 hpf were collected and anaesthetized with an anesthetic (ethyl 3-amino-benzoate methanesulfonate, CAS: 886–86–2) and then washed three times with PBS. o-Dianisidine (ODA, 0.6 mg/mL; Sigma, USA) was activated by 30% H₂O₂ in sodium acetate (10 mM, pH 5.2) and ethanol (4%) in the dark for 30 min. The stained zebrafish larvae were washed with PBS three times for 10 min each time. Fifteen stained zebrafish larvae were randomly selected from each group and examined under a microscope (Ming Mei Shot). The area of congestion in the atrium, ventricle, and pericardium of zebrafish was observed under a microscope and photographed. The area of congestion was quantitatively analyzed using the Image J software.

2.9. Acridine orange staining

The apoptosis signal of zebrafish larva heart was detected via acridine orange (AO) staining. After 96 h of exposure, 15 zebrafish larvae were randomly selected from each concentration group, including the DMSO group, for anesthesia and washed with PBS three times for 5 min each. The larvae were purged three times with 30% (v/v) Danieau's solution (58 mM of NaCl, 0.7 mM of KCl, 0.4 mM of MgSO₄, 0.6 mM of Ca(NO₃)₂, and 5 mM of HEPES; pH 7.4), transferred to 30% Danieau's solution containing 5 μ g/mL AO, and incubated for 20 min. Cell apoptosis was observed under a microscope (Ming Mei Shot). The fluorescence intensity of individual larva was quantitatively measured by measuring the integrated optical density area by using the Image J software.

2.10. Statistics

Heart rate, cardiac malformation rate, pericardium area, heart area, congestion area, and apoptosis fluorescence measurement levels were statistically analyzed by one-way ANOVA. Dunnett's test was performed to determine mean differences between the control and exposure treatment groups (SPSS Statistics 25.0). All data were considered normal on the basis of Kolmogorov–Smirnov one-sample test and Levene's test. Significant differences versus control are indicated as * $P < 0.05$, ** $P < 0.01$, and *** $P < 0.0001$.

3. Results

3.1. Effects of different MZ concentrations on pericardial cavity area

The zebrafish embryos were exposed to different MZ concentrations from 4 hpf to 96 hpf. The pericardial cavity was photographed at the same magnification, and the area of the pericardial cavity at each MZ exposure concentration was quantitatively analyzed. No zebrafish heart malformation was noted in the control group (Afouda et al., 2020) (Fig. 1A-a). However, in the exposed groups, cardiotoxic effects, such as pericardial edema, cardiac congestion, and myocardial fibrosis, were observed in the heart of the zebrafish larvae. Moreover, as exposure concentration increase, the toxic effects became more severe (Fig. 1A-b–e and Fig.A.1). The incidence of zebrafish heart abnormalities also increased with the increase in exposure concentration, and the difference between each exposure group and the control group was statistically significant ($p < 0.01$) (Fig. 1B). Quantitative statistics of zebrafish pericardial area under each exposure concentration showed that the difference between the low concentration group (1.88 and 2.81 μ M) and the control group was not statistically significant, whereas the difference between the high concentration group (3.76 and 7.52 μ M) and the control group was no statistically significant ($p < 0.01$) (Fig. 1C). The heart rate of the zebrafish decreased with the increase in exposure concentration. Except for the lowest exposure concentration group, the difference between the other exposure concentration groups and the

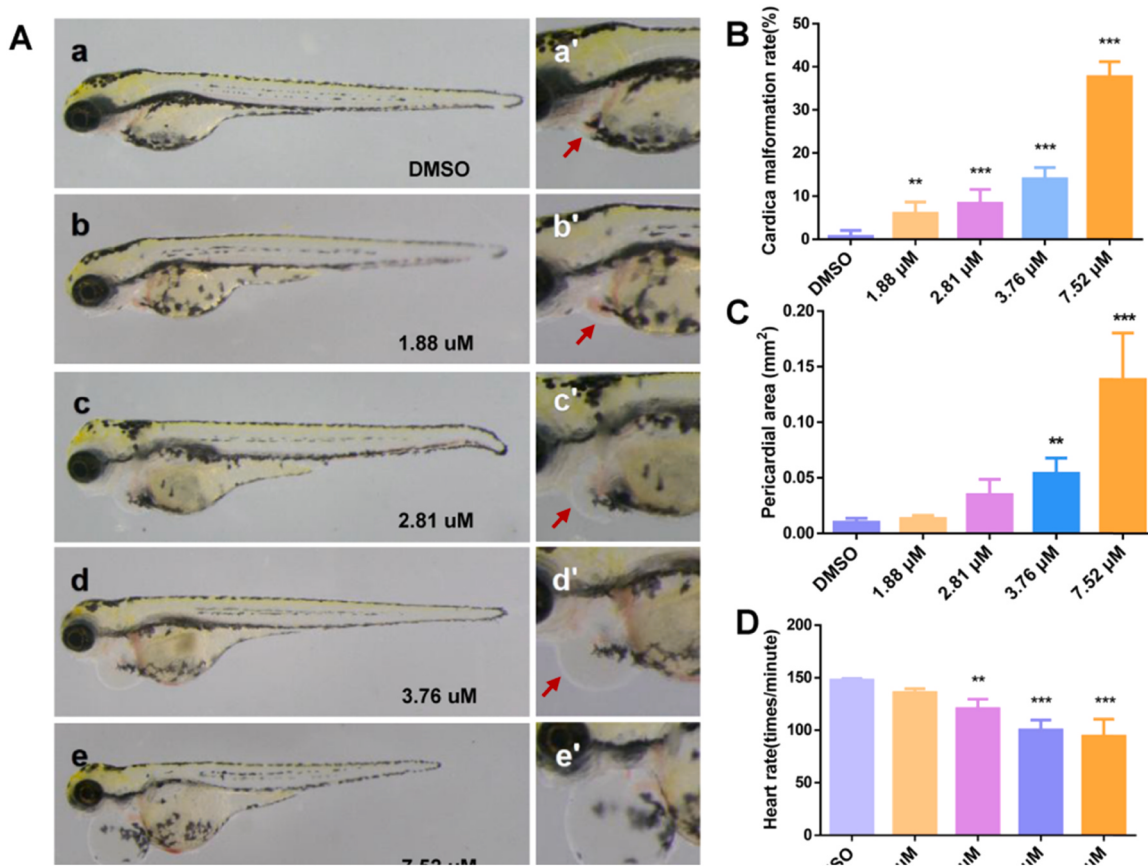


Fig. 1. Phenotype of MZ-treated zebrafish larvae. (A) a–e is the heart at $2.5\times$ magnification, and a'–e' is the heart at $5.0\times$ magnification. (B–D) Malformation rate, pericardial edema, and heart rate of zebrafish larva heart, respectively. The pericardium is indicated by the red arrow. An asterisk (*) indicates a significant difference ($p < 0.05$) between the treatment groups and the control group (** $p < 0.01$; *** $p < 0.001$). n = 15 larvae per group. (For interpretation of the references to colour in this figure legend, the reader is referred to the web version of this article.)

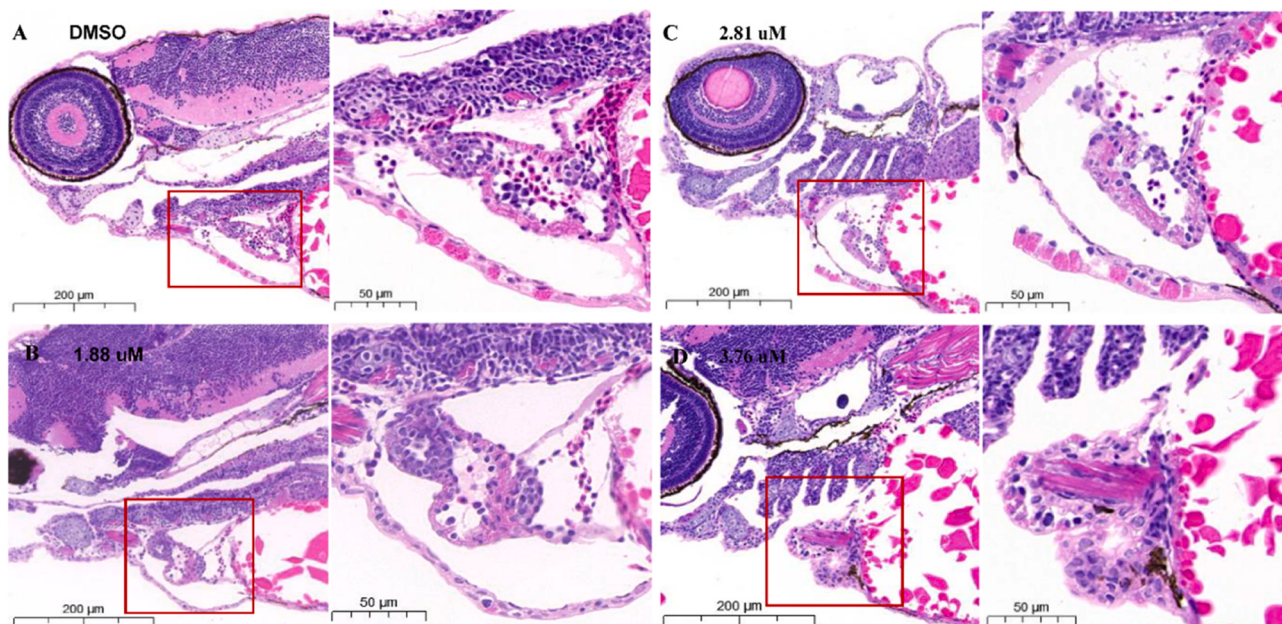


Fig. 2. Representative images reflecting the effects of different MZ concentrations on heart tissues in zebrafish at 96 hpf. n = 15 larvae per group.

control group was statistically significant ($p < 0.01$) (Fig. 1D).

3.2. Effects of different MZ concentrations on zebrafish heart tissue

In the control group, the heart size was moderate, the morphology of myocardial cells was normal, the ventricular wall was evenly distributed, and the heart cavity was filled with red blood cells (Fig. 2A). However, in the exposed groups, the heart size and myocardial cell nuclei were deeply stained and eosinophilic, the ventricular wall was thickened, the volume of red blood cells was substantially reduced, and the heart had obvious vacuolar changes (Fig. 2B–D). When the MZ concentration was $2.81 \mu\text{M}$, the zebrafish larvae had vacuolar changes in the heart and reduced red blood cells in the heart cavity (Fig. 2C). At $3.76 \mu\text{M}$, heart fibrosis was severe, heart volume was reduced, and the entire heart cavity was almost atresia (Fig. 2D).

3.3. Effects of different MZ concentrations on heart area

After ODA staining, the pericardial cavity of the zebrafish larvae at 96 hpf was imaged at the same magnification, and the heart area at each concentration was quantitatively analyzed. As the dose of MZ increased, the area of the zebrafish heart gradually decreased (Fig. 3 A). Results of quantitative analysis showed that the heart area of each exposure group was smaller than that of the control group ($P < 0.001$) (Fig. 3 C). Nevertheless, the area of congestion below the heart gradually increased (Fig. 3 A). Compared with that of the control group, the hyperemia area of each concentration group was statistically significant ($P < 0.001$) (Fig. 3B).

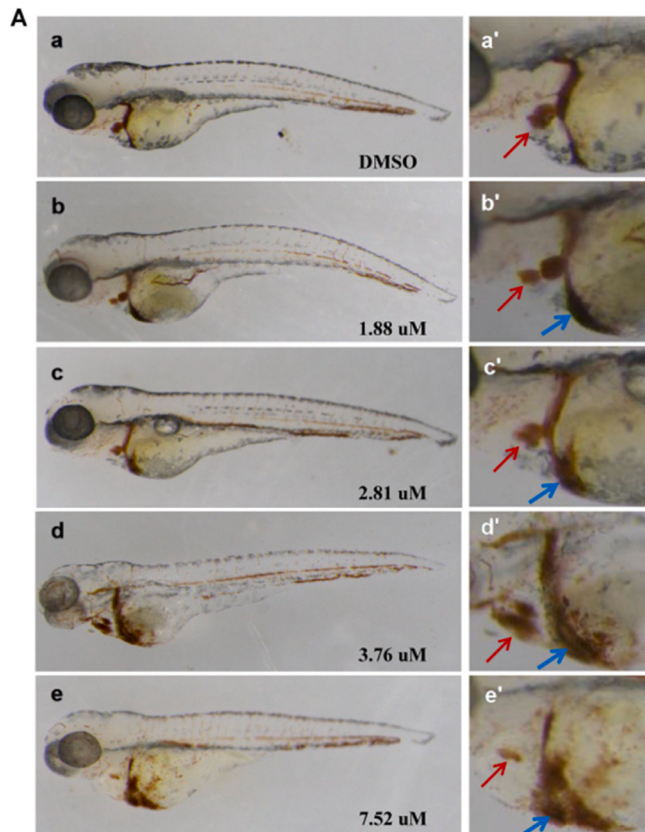


Fig. 3. Effects of exposure to different MZ concentrations at 96 hpf on the cardiac developmental toxicity of zebrafish. (A) a–e is the heart at $2.5\times$ magnification, and a '–e' is the heart at $5.0\times$ magnification. The atrium and the ventricle are indicated by the red arrow, whereas the area of congestion is indicated by the blue arrow. (B) Results of quantitative statistical analysis of cardiac congestion in each concentration group. (C) Results of quantitative analysis of ventricle and atrium area in each concentration group. An asterisk (*) indicates a significant difference ($p < 0.05$) between the treatment groups and the control group (* $p < 0.01$; ** $p < 0.001$). $n = 15$ larvae per group. (For interpretation of the references to colour in this figure legend, the reader is referred to the web version of this article.)

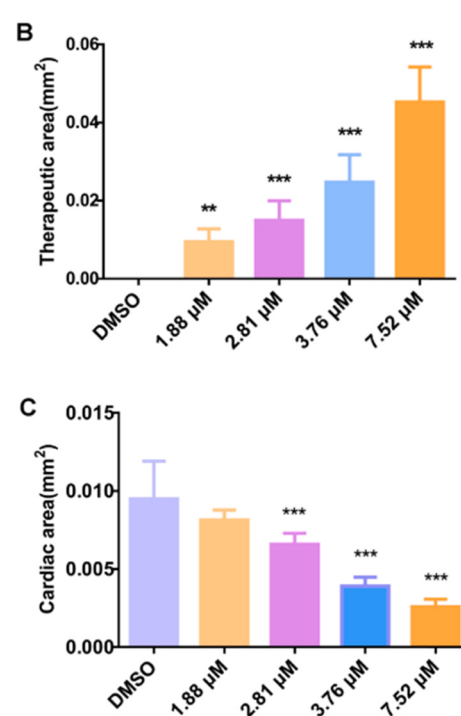
3.4. Transcriptomic analysis

Clean data were filtered and sequenced to obtain mapped data. Differential expression analysis, functional annotation, and functional enrichment analysis of DEGs were performed according to the expression level of the genes in different samples or sample groups. The results of quality control are shown in Fig. A2 B. According to the overall dispersion of expression levels, the expression level of each sample met the quality control requirements. Differences in gene expression levels between MZ ($3.0 \mu\text{M}$) and the control group were depicted using volcano plots (Fig. A2C). A total of 636 differential genes were obtained, 424 of which were upregulated and 212 were downregulated (Fig. A2 D).

Transcriptome sequencing detected thermograms of differential genes related to zebrafish heart development (Fig. 4 A). The Gene Ontology and Kyoto Encyclopedia of Genes and Genomes pathways of the DEGs were enriched using the R package clusterProfiler (Matthews et al., 2002). Compared with the genome-wide background, hypergeometric tests were performed to search for significantly enriched GO entries (Fig. 4B) and significantly enriched KEGG pathways (Fig. 4 C). According to the enrichment results of GO function analysis and KEGG pathway enrichment, systematic analysis revealed three main pathways related to zebrafish cardiac developmental toxicity, namely, Notch, P53, and apoptosis signaling pathways (Fig. 4C).

3.5. MZ exposure activated the Notch signaling pathway

The Notch signaling pathway was found to affect zebrafish heart development by regulating the upregulation of *osm*, *pfkfb3*, *foxh1*, and



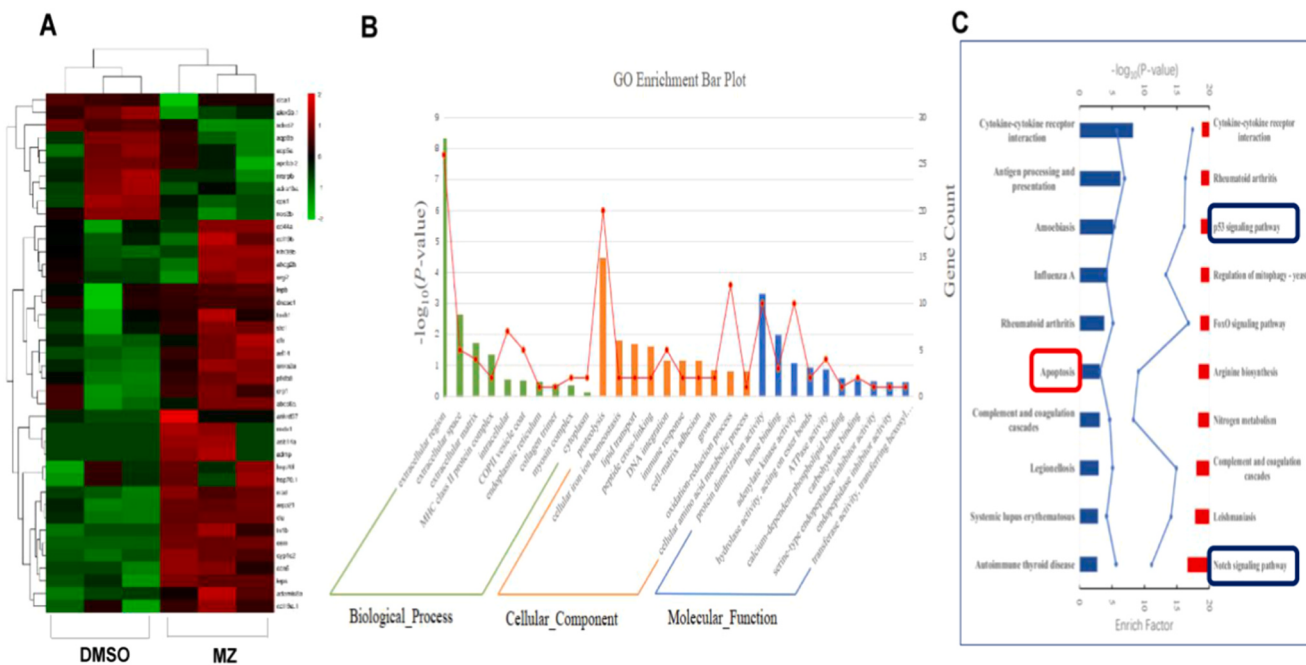


Fig. 4. GO functional analysis and KEGG pathways of different genes. (A) Transcriptome heat map of DEGs related to zebrafish cardiotoxicity after exposure to MZ at 96 h. (B) GO function annotation and enrichment analysis (control vs. MZ). GO analysis includes biological processes, cell components, and molecular functions. Dots on the line graph indicate the number of DEGs in each GO item. The size of the dots represents the number of differential genes, and the color expresses the *p* value. (C) Differentially gene-enriched KEGG pathways; pathways on the left (blue bar) are enriched by downregulated genes, whereas pathways on the right (red bar) are enriched by upregulated genes. The X- and Y-axes represent the pathway's name and rich factor, respectively. The pathway circled here is related to the developmental toxicity of zebrafish heart. (For interpretation of the references to colour in this figure legend, the reader is referred to the web version of this article.)

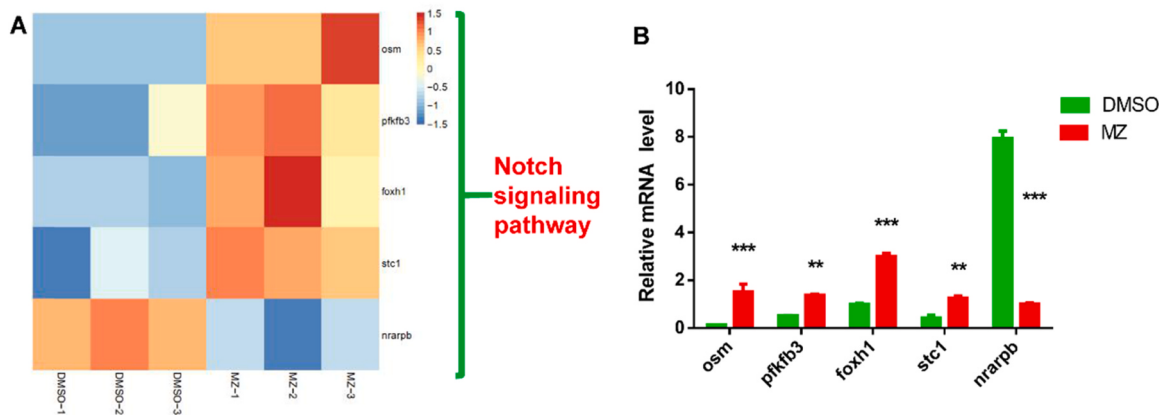


Fig. 5. Expression and verification of key genes in the Notch signaling pathway. (A) Heat map profiles of differential genes (*osm*, *ptkfb3*, *foxh1*, *stc1*, and *nrarpb*) related to the Notch signaling pathway. (B) mRNA relative expression levels of the genes related to the Notch signaling pathway were detected by qPCR. Each value represents the mean \pm SD from at least three independent experiments ($n = 3$). An asterisk (*) indicates a significant difference ($p < 0.05$) between the treatment groups and the control group (** $p < 0.01$; *** $p < 0.001$).

stc1 genes and the downregulation of *nrarpb* (Fig. 5A). The reliability of transcriptome results was verified via RT-qPCR validation on key genes of the Notch signaling pathway compared with that in the experimental group. The relative mRNA expression levels of *osm*, *ptkfb3*, *foxh1*, and *stc1* genes were all upregulated, whereas that of *nrarpb* was downregulated. These results were consistent with those of transcriptome analysis (Fig. 5B).

3.6. Apoptosis-related signal pathways and apoptosis signal detection

Results of enrichment analysis of the DEGs also revealed that estrogen metabolism-related genes (i.e., *hsp70.1*, *hsp70.2*, and *hsp70l*) and P450 metabolism family genes (*cyp1c2* and *cyp3c3*) were upregulated in

the exposure groups (Fig. 6 A). Enrichment of the KEGG pathway indicated that the cytochrome P450 metabolic pathway was statistically significant in both the MZ treatment and control groups ($p < 0.05$) (Table A2). Random selection of *cyp1c2*, *hsp70l*, and *lepb* was verified by RT-qPCR. The expression levels of these genes were upregulated, consistent with the results of transcriptome sequencing (Fig. 6B). Both estrogen receptor activation and P450 metabolic pathways are related to zebrafish cardiomyocyte apoptosis. AO staining results also verified that zebrafish cardiac developmental toxicity was found to be related to apoptosis. In AO staining, the hearts of the zebrafish larvae in the control group did not produce green fluorescence (Fig. 6C-a). By contrast, the hearts of the zebrafish larvae in MZ treatments of 1.88, 2.81, 3.76, and 7.52 μ M produced a bright green fluorescence, which indicated the

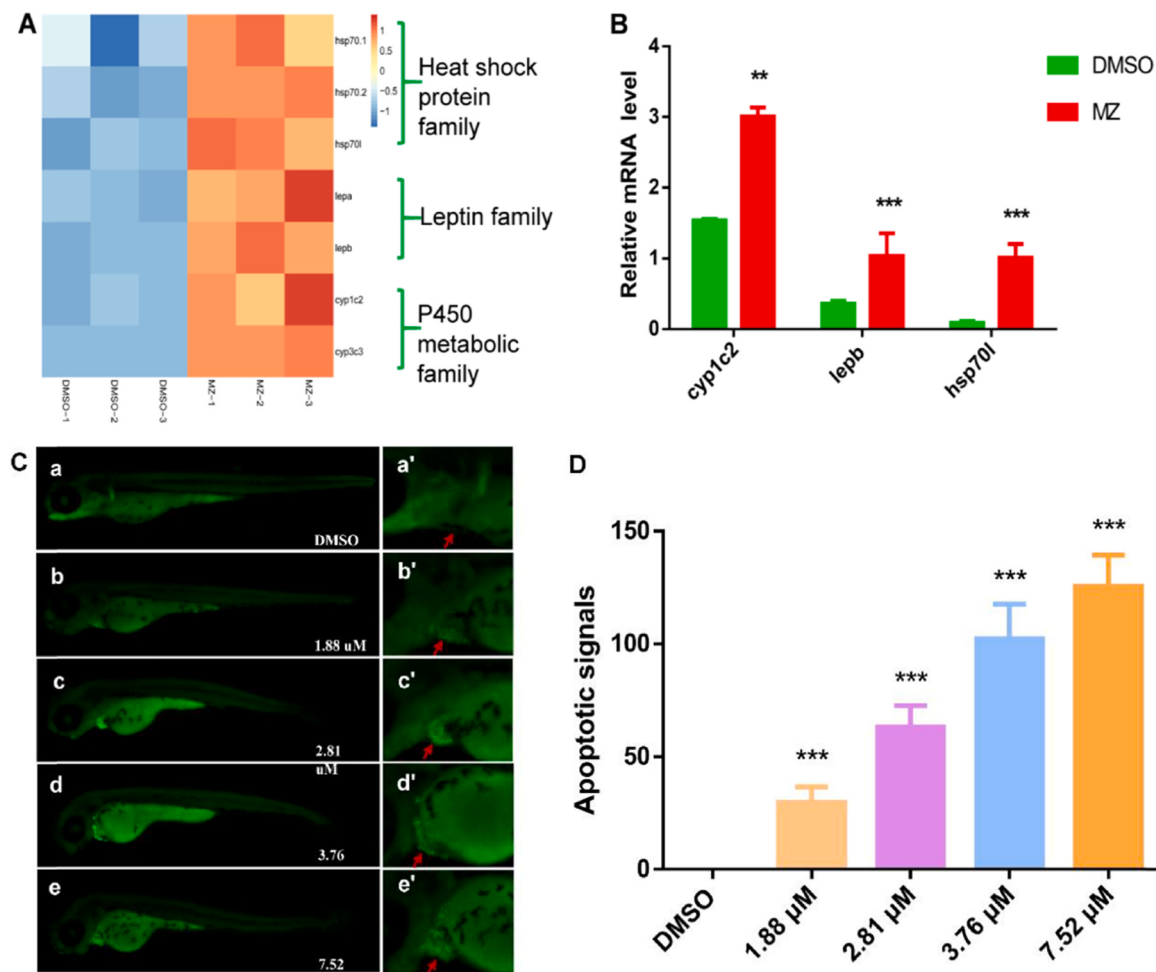


Fig. 6. The possible mechanism of MZ-mediated cardiomyocyte apoptosis. (A) The heat map showed that the genes related to the P450 metabolic family and the estrogen signaling pathway were upregulated in the exposure group (3.0 μ M). (B) Relative mRNA expression level of the three selected genes with different expression profiles from the results of RNA-seq. (C) MZ induced apoptosis in the zebrafish larvae at 96 hpf as detected by acridine orange (AO) staining. The red arrow marks the apoptotic signal. (D) Relative fluorescence of region with bright spots in AO staining as quantified using Image J. An asterisk (*) indicates a significant difference ($p < 0.05$) between the treatment groups and the control group (** $p < 0.01$; *** $p < 0.001$). n = 15 larvae per group.

presence of apoptotic cells (Fig. 6C b–e). Results of quantitative analysis revealed that the apoptosis signal of zebrafish larva heart in each MZ concentration was statistically significant compared with that in the control group (Figs. 6D and A3) ($P < 0.001$).

4. Discussion

The detrimental effects of MZ to health have been extensively studied. However, whether MZ has cardiotoxicity is unclear. In this study, MZ induced a series of toxic effects on cardiac development, including pericardial edema, heart rate reduction, cardiac congestion, and myocardial fibrosis, in zebrafish embryos. Transcriptomics and bioinformatics methods are tools for studying the toxicity mechanism of pollutants (Mu et al., 2018). By integrating the results of transcriptome sequencing analysis and the phenotypes of zebrafish heart malformation, we explored the possible mechanism by which MZ induces zebrafish heart malformation. Transcriptome sequencing analysis revealed that the Notch signaling and apoptosis-related pathways were related to the cardiotoxicity induced by MZ in zebrafish larvae.

The Notch signaling pathway, which is composed of five ligands (i.e., delta-like1, delta-like3, delta-like4, Jagged1, and Jagged2) and four Notch receptors (Notch1–4), plays an important role in heart development (Dergilev et al., 2018). The Notch pathway is complicated, mainly composed of three parts: Notch receptor, Notch ligand and downstream

target genes (Okazaki et al., 2020). Changes in any one of these factors will affect the transmission of the Notch signaling pathway (Dergilev et al., 2018). The level of Notch signal in cardiomyocytes decreases with development after birth, but it is reactivated after injury (Gude et al., 2008; Zeng et al., 2016). The activation abnormality of Notch signaling pathway is related to myocardial infarction (Kratsios et al., 2010; Salguero-Jiménez et al., 2018; Li et al., 2010). Changes in the NOTCH signal in the endocardium lead to congenital structural malformations, which can lead to heart disease in newborns and adults (Luxán et al., 2016). MZ-treated zebrafish research experiments show that the genes related to the Notch signaling pathway, namely, *osm*, *pfkfb3*, *foxb1*, *stc1*, and *nrarpb*, were differently expressed between the control group and the MZ treatment groups. Except for *nrarpb*, which was downregulated in the MZ treatment groups, the other genes (*osm*, *pfkfb3*, *foxb1*, and *stc1*) were upregulated, consistent with the results of RT-qPCR verification.

Oncostatin M (*osm*) is an inflammatory cytokine (Gruson et al., 2017) and associates with cardiac hypertrophy and cardiac inflammatory disease (M. Li et al., 2020; Y. Li et al., 2020). *Osm* can inhibit cardiomyocyte apoptosis and promote cardiomyocyte differentiation through the Notch signaling pathway (Ikeda et al., 2019; Li et al., 2019; Zhang et al., 2015). MZ lead to a high expression of *osm* in our results, which may be responsible for the cardiac hypertrophy of zebrafish. *Pfkfb3* has been shown to be involved in a variety of physiological and

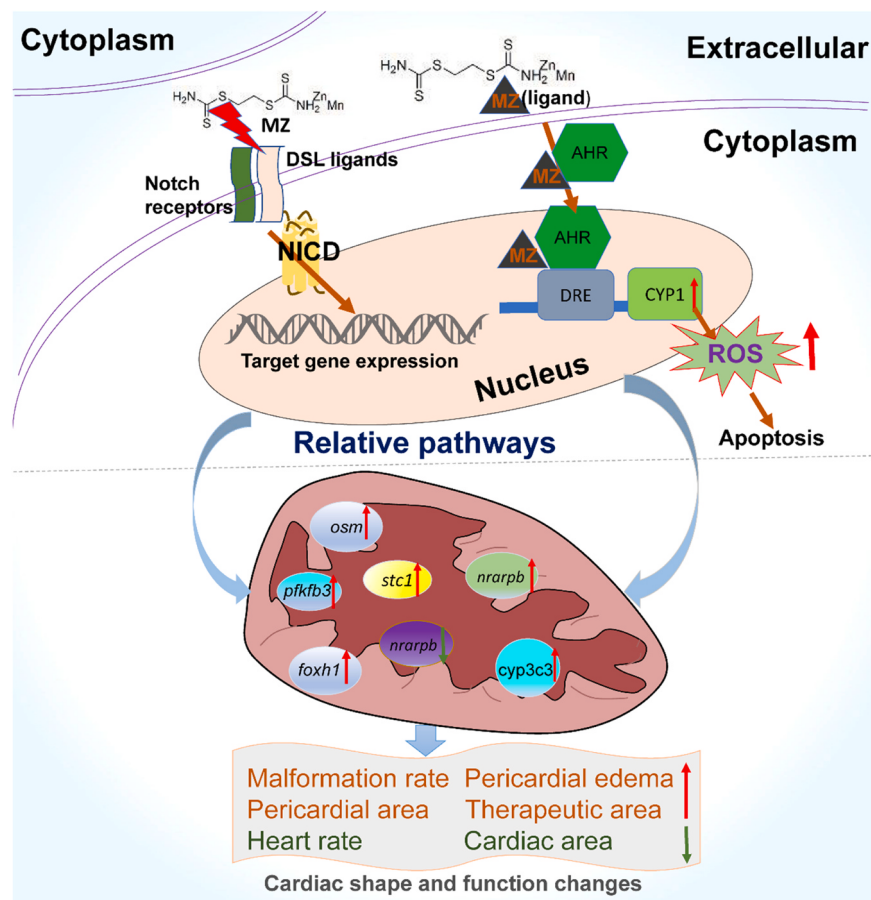


Fig. 7. Predictive regulatory mechanism for MZ exposure on zebrafish cardiotoxicity. Notch receptors (Notch1–4), DSL ligands (delta-like1, delta-like3, delta-like4, Jagged1, and Jagged2).

pathological processes, including angiogenesis, atherosclerosis, pulmonary fibrosis and cardiac dysfunction (Tian et al., 2019). And *pdkfb3* is involved in the regulation of angiogenesis through the Notch signaling pathway (Zheng et al., 2018). Consistent with the previous study (Tian et al., 2019), in this study, mRNA-seq analysis and RT-qPCR data highlighted the up-regulated expression of *pdkfb3* in MZ exposed zebrafish heart tissue, which suggests that *pdkfb3* may be related to MZ-induced cardiac dysfunction in zebrafish.

The *foxh1* transcription factor acts as a nodal signal connecting the Wnt and Notch pathways and mediates cardiac developmental asymmetry (Tanaka et al., 2014; Afouda et al., 2020; Lenhart et al., 2013). *Foxh1* is expressed only during early development in mouse (Afouda et al., 2020), xenopus (Afouda et al., 2020) and zebrafish (Attisano et al., 2001). Previous studies have reported that overexpression of *foxh1* has a negative effect on the cardiovascular system formation in zebrafish embryos (Choi et al., 2007), this is consistent with our study, in which the *foxh1* gene expression in zebrafish exposed to MZ was up-regulated, which may be related to the cardiac toxicity of zebrafish induced by MZ. The expression of *stc1* is elevated in the heart tissues of patients with amyloidosis (AL) cardiomyopathy. Overexpression of *stc1* in the myocardium can lead to increased reactive oxygen species production, contractile dysfunction, and ultimately cardiac insufficiency (Guan et al., 2013). *Stc1* gene silencing can prevent AL-LC(Immunoglobulin light chain)-induced cardiotoxicity in cardiomyocytes and protect zebrafish from AL-LC-induced cell death and early death. *Stc1* is also a nonclassical receptor of the Notch signaling pathway (Li et al., 2018). Notch-regulated ankyrin repeat protein (*nrarpb*) can connect the Notch and Wnt signaling pathways in endothelial cells, thereby regulating the stability of new blood vessel connections in zebrafish tissues. DLL4

/Notch induces *nrarpb* expression in endothelial stalk cells, restricts the Notch signaling pathway, and promotes the Wnt signaling pathway (Dasmahapatra et al., 2019; Phng et al., 2009). Previous reports show that the downregulation of *nrarpb* in zebrafish caused pericardial edema and reduction of the heart rate (Dasmahapatra et al., 2019). These results are consistent with the present study. we infer that MZ-induced cardiac teratogenic effects may be partly due to *nrarpb* expression downregulation affects the connection between the Notch and Wnt signaling pathways. However, further research is needed to be explored.

The P53 and apoptosis signaling pathways are statistically different between the MZ treatment groups and the control group ($P < 0.05$). Apoptosis plays an important role in the occurrence and development of cardiovascular diseases, such as ischemic heart disease and recurrent cardiovascular disease. Perfusion injury, cardiomyopathy caused by chemotherapy, and heart failure are all related to cell apoptosis (Del Re et al., 2019; Haunstetter and Izumo, 1998).

Enrichment of KEGG pathways and DEGs found that apoptosis-related pathways also mediated MZ-induced zebrafish cardiotoxicity through the intracellular apoptotic pathway. The results of KEGG pathway enrichment showed that the P450 metabolic family participated in the zebrafish cardiotoxicity observed in this study (Table S2).

The aryl hydrocarbon receptor (AhR) is a ligand-activated transcription factor that can be activated by a wide range of environmental chemicals, such as polycyclic aromatic hydrocarbons and dioxin-like compounds (Shankar et al., 2020), and regulates the expression of p450 family genes. In the absence of ligand, AhR remains in the cytoplasm by binding to chaperone molecules. Upon ligand binding, AhR migrates into the nucleus and consequently stimulates the transcription of target genes. Which includes cytochrome P450 enzymes (CYP1B1,

CYP1A1, CYP1A2) (Shankar et al., 2020; Toydemir et al., 2021). It is reported that the up-regulation of P450 gene will increase the release of ROS to induce apoptosis (Granville et al., 2004; Liu et al., 2019). Studies also have shown that MZ activate the AhR signaling pathway to regulate the up-regulation of CYP expression (Lori et al., 2021; Pariseau et al., 2011). AhR-mediated developmental toxicity can cause zebrafish cardiomyocyte apoptosis and cardiac malformation phenotype (Bugiak and Weber, 2010; Guan et al., 2019). These results indicate that MZ may act as a ligand of AhR to activate the AhR signaling pathway and affect heart development. That increases the expression of target genes (*cyp1c2* and *cyp3c3*) to generate more ROS and promotes cardiomyocyte apoptosis (Ehrlich et al., 2020). Therefore, we infer that MZ-induced cardiac teratogenic effects may be partly due to the AhR pathway.

Furthermore, the DEGs showed that the expression of (i.e., *hsp70.1*, *hsp70l* and *hsp70.2*) was substantially upregulated in the MZ treatment groups, as verified by RT-qPCR. Heat shock proteins (HSPs) are induced in response to various stresses and to protect cells from such stresses, including apoptosis-inducing stimuli (Gotoh and Terada, 2001). *In vitro* and *in vivo* studies have shown that *hsp70* has a regulatory role in the development of the heart (He et al., 2021; Peng et al., 2020). Animal researches have shown that *hsp70-1* transgenic or knockout mice can resist UVB radiation and cause serious cardiac dysfunction (Song et al., 2019; Hampton et al., 2003). Knocking out *hsp70* genes might induce serious cardiac dysfunction (Kumar et al., 2016). Increased *hsp70*, by interacting at several points on apoptotic signaling pathways, leads to inhibition of apoptosis (Zhai et al., 2019). Previous research demonstrated that MZ can induce zebrafish larvae to produce ROS, which leads to cell apoptosis (Paganotto Leandro et al., 2021). Study also found that ROS can trigger the up-regulation of *hsp70* to achieve a protective mechanism for cells (Rao et al., 2018). Consistent with our results, we inferred that the upregulation of *hsp70* (*hsp70.1*, *hsp70l* and *hsp70.2*) may be due to ROS-induced zebrafish cardiomyocyte apoptosis, which triggered the general protective mechanism of heat shock protein family to the cardiomyocytes.

The leptin hormone relates to multiple system functions, such as immune response, energy expenditure, hematopoiesis, and angiogenesis (Himms-Hagen, 1999). Clinical data shows that leptin is associated with cardiovascular morbidity, such as heart failure (HF) and acute myocardial infarction (MI). Leifheit-Nestler et al. (2013). Inhibition of leptin activity could preserve myocardial function in rats with acute MI (Moro et al., 2011), and increasing leptin synthesis can promote cardiomyocyte hypertrophy and fibrosis, and enhance myocardial dysfunction (Kain et al., 2018). Leptin which increases ROS production, promotes TGF β synthesis to mediates apoptosis and promotes myocardial fibrosis (Pardali et al., 2017). Our results are consistent with these findings. Therefore, we conclude that MZ-induced myocardial hypertrophy and apoptosis may be partly attributed to excessive leptin availability. The mechanism by which apoptosis-related pathways lead to increased expression of cardiac apoptotic signals in zebrafish was verified by the results of AO staining.

Although we have revealed the possible mechanism of MZ cardiotoxicity through transcriptomics analysis, our experimental design still has certain limitations. This experiment explores the effect of MZ exposure on zebrafish heart development during embryonic period. At this time, the individual zebrafish larvae are extremely small, therefore, there are technical difficulties in separating the heart of zebrafish at 96 hpf to perform accurate mechanism research.

5. Conclusion

Our findings demonstrated, for the first time, MZ exposure during early embryonic development can cause cardiac developmental toxicity in zebrafish embryos. And MZ induced cardiac developmental toxicity in zebrafish embryos may be related to the activation of Notch signaling pathway and apoptosis-related pathways. In summary, our findings emphasize the potential health risks involved in application of MZ.

CRediT authorship contribution statement

Yongfeng Wang: Methodology, Software, Visualization, Writing – review & editing. **Zhiqian Yu:** Methodology, Software, Visualization. **Zunpan Fan:** Methodology. **Methodology.** **Yiwei Fang:Liting He:** Methodology, Software. **Meilin Peng:** Methodology. **Yuanyao Chen:** Methodology, Data curation. **Zhiyong Hu:** Conceptualization, Data curation. **Kai Zhao:** Conceptualization, Data curation. **Huiping Zhang:** Conceptualization, Supervision, Writing – review & editing. **Chunyan Liu:** Conceptualization, Supervision, Writing – review & editing.

Declaration of Competing Interest

The authors declare that we have no known competing financial interests or personal relationships that could have appeared to influence the work reported in this paper.

Acknowledgments

This work was funded by the National Key R&D Program of China (Project No: 2018YFC1004300, 2018YFC1004304).

Declaration of competing interest

The authors declare that they have no known competing financial interests or personal relationships that could have appeared to influence the work reported in this paper.

Appendix A. Supporting information

Supplementary data associated with this article can be found in the online version at doi:10.1016/j.ecoenv.2021.112798.

References

- Afouda, B.A., Nakamura, Y., Shaw, S., Charney, R.M., Paraiso, K.D., Blitz, I.L., Cho, K., Hoppler, S., 2020. Foxh1/nodal defines context-specific direct maternal Wnt/ β -catenin target gene regulation in early development. iScience 23 (7), 101314.
- Anders, S., Huber, W., 2010. Differential expression analysis for sequence count data. Genome Biol. 11 (10), 106.
- Asparch, Y., Svartz, G., Pérez, C.O.L.L.C., 2020. Toxicity characterization and environmental risk assessment of Mancozeb on the South American common toad Rhinella arenarum. Environ. Sci. Pollut. Res. Int. 27 (3), 3034–3042.
- Attisano, L., Silvestri, C., Izzi, L., Labbé, E., 2001. The transcriptional role of Smads and FAST (FoxH1) in TGFbeta and activin signalling. Mol. Cell Endocrinol. 180 (1–2), 3–11.
- Bianchi, S., Nottola, S.A., Torge, D., Palmerini, M.G., Necozione, S., Macchiarelli, G., 2020. Association between female reproductive health and mancozeb: systematic review of experimental models. Int. J. Environ. Res. Public Health 17 (7), 2580.
- Bugiak, B.J., Weber, L.P., 2010. Phenotypic anchoring of gene expression after developmental exposure to aryl hydrocarbon receptor ligands in zebrafish. Aquat. Toxicol. 99 (3), 423–437.
- Casida, J.E., 2017. Why prodrugs and propesticides succeed. Chem. Res. Toxicol. 30 (5), 1117–1126.
- Choi, J., Dong, L., Ahn, J., Dao, D., Hammerschmidt, M., Chen, J.N., 2007. FoxH1 negatively modulates flk1 gene expression and vascular formation in zebrafish. Dev. Biol. 304 (2), 735–744.
- Costa-Silva, D., Leandro, L.P., Vieira, P.B., de Carvalho, N.R., Lopes, A.R., Schimith, L.E., Nunes, M., de Mello, R.S., Martins, I.K., de Paula, A.A., Cañedo, A.D., Moreira, J., Posser, T., Franco, J.L., 2018. N-acetylcysteine inhibits Mancozeb-induced impairments to the normal development of zebrafish embryos. Neurotoxicol. Teratol. 68, 1–12.
- Dasmahapatra, A.K., Dasari, T.P.S., Tchounwou, P.B., 2019. Graphene-based nanomaterials toxicity in fish. Rev. Environ. Contam. Toxicol. 247, 1–58.
- Dergilev, K.V., Zubkova, E.S., Beloglazova, I.B., Menshikov, M.Y., Parfyonova, E.V., 2018. Notch signal pathway - therapeutic target for regulation of reparative processes in the heart. Ter. arkhiv 90 (12), 112–121.
- Ehrlich, A.M., Pacheco, A.R., Henrick, B.M., Taft, D., Xu, G., Huda, M.N., Mishchuk, D., Goodson, M.L., Slupsky, C., Barile, D., Lebrilla, C.B., Stephensen, C.B., Mills, D.A., Raybould, H.E., 2020. Indole-3-lactic acid associated with *Bifidobacterium*-dominated microbiota significantly decreases inflammation in intestinal epithelial cells. BMC Microbiol. 20 (1), 357.
- Genge, C.E., Lin, E., Lee, L., Sheng, X., Rayani, K., Gunawan, M., Stevens, C.M., Li, A.Y., Talab, S.S., Clayton, T.W., Hove-Madsen, L., Tibbits, G.F., 2016. The zebrafish heart

- as a model of mammalian cardiac function. *Rev. Physiol., Biochem. Pharmacol.* 171, 99–136.
- Gotoh, T., Terada, K., 2001. MORI M. hsp70-DnaJ chaperone pairs prevent nitric oxide-mediated apoptosis in RAW 264.7 macrophages. *Cell Death Differ.* 8 (4), 357–366.
- Granville, D.J., Tashakkor, B., Takeuchi, C., Gustafsson, A.B., Huang, C., Sayen, M.R., Wentworth P, Jr, Yeager, M., Gottlieb, R.A., 2004. Reduction of ischemia and reperfusion-induced myocardial damage by cytochrome P450 inhibitors. *Proc. Natl. Acad. Sci. USA* 101 (S), 1321–1326.
- Gruson, D., Ferracin, B., Ahn, S.A., Rousseau, M.F., 2017. Elevation of plasma oncostatin M in heart failure. *Future Cardiol.* 13 (3), 219–227.
- Guan, J., Mishra, S., Shi, J., Plovie, E., Qiu, Y., Cao, X., Gianni, D., Jiang, B., Del Monte, F., Connors, L.H., Seldin, D.C., Lavatelli, F., Rognoni, P., Palladini, G., Merlini, G., Falk, R.H., Semigran, M.J., Dec GW, Jr, Macrae, C.A., Liao, R., 2013. Stanniocalcin1 is a key mediator of amyloidogenic light chain induced cardiotoxicity. *Basic Res. Cardiol.* 108 (5), 378.
- Guan, F., Yang, X., Li, J., Dong, W., Zhang, X., Liu, N., Gao, S., Wang, J., Zhang, L., Lu, D., 2019. New molecular mechanism underlying Myc-mediated cytochrome P450 2E1 upregulation in apoptosis and energy metabolism in the myocardium. *J. Am. Heart Assoc.* 8 (1), 009871.
- Gude, N.A., Emmanuel, G., Wu, W., Cottage, C.T., Fischer, K., Quijada, P., Muraski, J.A., Alvarez, R., Rubio, M., Schaefer, E., Sussman, M.A., 2008. Activation of notch-mediated protective signaling in the myocardium. *Circ. Res.* 102 (9), 1025–1035.
- Gullino M.L., Tinivella F., Garibaldi A., et al. Mancozeb: Past, Present, and future. *Plant disease*, 2010, 94(9): 1076–1087.
- Hampton, C.R., Shimamoto, A., Rothnie, C.L., Griscavage-Ennis, J., Chong, A., Dix, D.J., Verrier, E.D., Pohlman, T.H., 2003. HSP70.1 and -70.3 are required for late-phase protection induced by ischemic preconditioning of mouse hearts [J]. *Am. J. Physiol. Heart Circ. Physiol.* 285 (2), H866–H874.
- Haunstetter, A., Izumo, S., 1998. Apoptosis: basic mechanisms and implications for cardiovascular disease. *Circ. Res.* 82 (11), 1111–1129.
- He, L., Chen, Y., Hu, Z., Zhang, Y., Wang, Y., Wei, J., Fan, Z., Xu, J., Peng, M., Zhao, K., Zhang, H., Liu, C., 2021. Evaluation of 3,4,4,9-trichlorocarbanilide to zebrafish developmental toxicity based on transcriptomics analysis. *Chemosphere* 278, 130349.
- Himms-Hagen, J., 1999. Physiological roles of the leptin endocrine system: differences between mice and humans. *Crit. Rev. Clin. Lab. Sci.* 36 (6), 575–655.
- Huang, M., Jiao, J., Wang, J., Xia, Z., Zhang, Y., 2018. Characterization of acrylamide-induced oxidative stress and cardiovascular toxicity in zebrafish embryos. *J. Hazard. Mater.* 347, 451–460.
- Hwang, E.S., Cash, J.N., Zabik, M.J., 2001. Postharvest treatments for the reduction of mancozeb in fresh apples. *J. Agric. Food Chem.* 49 (6), 3127–3132.
- Ikeda, S., Mizushima, W., Sciarretta, S., Abdellatif, M., Zhai, P., Mukai, R., Fefelova, N., Oka, S.I., Nakamura, M., Del Re, D.P., Farrance, I., Park, J.Y., Tian, B., Xie, L.H., Kumar, M., Hsu, C.P., Sadayappan, S., Shimokawa, H., Lim, D.S., Sadoshima, J., 2019. Hippo deficiency leads to cardiac dysfunction accompanied by cardiomyocyte dedifferentiation during pressure overload. *Circ. Res.* 124 (2), 292–305.
- Jenkins, K.J., Correa, A., Feinstein, J.A., Botto, L., Britt, A.E., Daniels, S.R., Elixson, M., Warnes, C.A., Webb, C.L., American Heart Association Council on Cardiovascular Disease in the, Y., 2007. Noninherited risk factors and congenital cardiovascular defects: current knowledge: a scientific statement from the American Heart Association Council on Cardiovascular Disease in the Young: endorsed by the American Academy of Pediatrics. *Circulation* 115 (23), 2995–3014.
- Ji, C., Yan, L., Chen, Y., Yue, S., Dong, Q., Chen, J., Zhao, M., 2019. Evaluation of the developmental toxicity of 2,7-dibromocarbazole to zebrafish based on transcriptomics assay. *J. Hazard. Mater.* 368, 514–522.
- Kain, D., Simon, A.J., Greenberg, A., Ben Zvi, D., Gilburd, B., Schneiderman, J., 2018. Cardiac leptin overexpression in the context of acute MI and reperfusion potentiates myocardial remodeling and left ventricular dysfunction. *PLoS One* 13 (10), 0203902.
- Kim, J., Swartz, M., Langlois, P., Romitti, P., Weyer, P., Mitchell, L., Luben, T., Ramakrishnan, A., Malik, S., Lupo, P., Feldkamp, M., Meyer, R., Winston, J., Reefhuis, J., Blossom, S., Bell, E., Agopian, A., 2017. Estimated maternal pesticide exposure from drinking water and heart defects in offspring. *Int. J. Environ. Res. Public Health* 14 (8), 889.
- Kratsios, P., Catela, C., Salimova, E., Huth, M., Berno, V., Rosenthal, N., Mourkioti, F., 2010. Distinct roles for cell-autonomous Notch signaling in cardiomyocytes of the embryonic and adult heart. *Circ. Res.* 106 (3), 559–572.
- Kumar, S., Stokes, J., Singh, U.P., Scissum Gunn, K., Acharya, A., Manne, U., Mishra, M., 2016. Targeting Hsp70: A possible therapy for cancer. *Cancer Lett.* 374 (1), 156–166.
- Leifheit-Nestler, M., Wagner, N.M., Gogiraju, R., Didié, M., Konstantinides, S., Hasenfuss, G., Schäfer, K., 2013. Importance of leptin signaling and signal transducer and activator of transcription-3 activation in mediating the cardiac hypertrophy associated with obesity. *J. Transl. Med.* 11, 170.
- Lenhart, K.F., Holtzman, N.G., Williams, J.R., Burdine, R.D., 2013. Integration of nodal and BMP signals in the heart requires FoxH1 to create left-right differences in cell migration rates that direct cardiac asymmetry. *PLoS Genet.* 9 (1), 1003109.
- Liu, H., Shi, L., Giesy, J.P., Yu, H., 2019. Polychlorinated diphenyl sulfides can induce ROS and genotoxicity via the AhR-CYP1A1 pathway. *Chemosphere* 223, 165–170.
- Liu, F., Wen, Z., 2002. Cloning and expression pattern of the lysozyme C gene in zebrafish. *Mech. Dev.* 113 (1), 69–72.
- Li, R., Baek, K.I., Chang, C.C., Zhou, B., Hsiai, T.K., 2019. Mechanosensitive pathways involved in cardiovascular development and homeostasis in zebrafish. *J. Vasc. Res.* 56 (6), 273–283.
- Li, Y., Feng, J., Song, S., Li, H., Yang, H., Zhou, B., Li, Y., Yue, Z., Lian, H., Liu, L., Hu, S., Nie, Y., 2020. gp130 controls cardiomyocyte proliferation and heart regeneration. *Circulation* 142 (10), 967–982.
- Li, Y., He, Z.C., Zhang, X.N., Liu, Q., Chen, C., Zhu, Z., Chen, Q., Shi, Y., Yao, X.H., Cui, Y., H., Zhang, X., Wang, Y., Kung, H.F., Ping, Y.F., Bian, X.W., 2018. Stanniocalcin-1 augments stem-like traits of glioblastoma cells through binding and activating NOTCH1. *Cancer Lett.* 416, 66–74.
- Li, Y., Hiroi, Y., Liao, J.K., 2010. Notch signaling as an important mediator of cardiac repair and regeneration after myocardial infarction. *Trends Cardiovasc. Med.* 20 (7), 228–231.
- Li, M., Yao, L., Chen, H., Ni, X., Xu, Y., Dong, W., Fang, M., Chen, D., Aowuliji, Xu, L., Zhao, B., Deng, J., Kwok, K.W., Yang, J., Dong, W., 2020. Chiral toxicity of muscone to embryonic zebrafish heart. *Aquat. Toxicol. (Amst., Neth.)* 222, 105451.
- Lori, G., Tassinari, R., Narciso L., et al. Toxicological Comparison of Mancozeb and Zoxamide Fungicides at Environmentally Relevant Concentrations by an In Vitro Approach. 2021, 18 (16): 8591.
- Luxán, G., D'amato, G., Macgrogan, D., de la Pompa, J.L., 2016. Endocardial notch signaling in cardiac development and disease. *Circ. Res.* 118 (1), e1–e18.
- Martin, K.E., Waxman, J.S., 2021. Atrial and sinoatrial node development in the zebrafish heart. *J. Cardiovasc. Dev. Dis.* 8 (2), 15.
- Matthews, M., Trevarrow, B., Matthews, J., 2002. A virtual tour of the guide for zebrafish users. *Lab Anim.* 31 (3), 34–40.
- Moore-Morris, T., Van Vliet, P.P., Andelfinger, G., Pucat, M., 2018. Role of epigenetics in cardiac development and congenital diseases. *Physiol. Rev.* 98 (4), 2453–2475.
- Mora, A.M., Córdoba, L., Cano, J.C., Hernandez-Bonilla, D., Pardo, L., Schnaas, L., Smith, D.R., Menezes-Filho, J.A., Mergler, D., Lindh, C.H., Eskenazi, B., van Wendel de Joode, B., 2018. Prenatal mancozeb exposure, excess manganese, and neurodevelopment at 1 Year of Age in the Infants' Environmental Health (ISA) study. *Environ. Health Perspect.* 126 (5), 057007.
- Moro, C., Grauzam, S., Ormezzano, O., Toufektsian, M.C., Tanguy, S., Calabrese, P., Coll, J.L., Bak, I., Juhasz, B., Tosaki, A., de Leiris, J., Boucher, F., 2011. Inhibition of cardiac leptin expression after infarction reduces subsequent dysfunction. *J. Cell. Mol. Med.* 15 (8), 1688–1694.
- Mu, X., Huang, Y., Li, X., Lei, Y., Teng, M., Li, X., Wang, C., Li, Y., 2018. Developmental effects and estrogenicity of bisphenol a alternatives in a zebrafish embryo model. *Environ. Sci. Technol.* 52 (5), 3222–3231.
- Nascimento, S., Baierle, M., Göethel, G., Barth, A., Brucker, N., Charão, M., Sauer, E., Gauer, B., Arbo, M.D., Altknecht, L., Jager, M., Dias, A.C., de Salles, J.F., Saint' Pierre, T., Gioda, A., Moresco, R., Garcia, S.C., 2016. Associations among environmental exposure to manganese, neuropsychological performance, oxidative damage and kidney biomarkers in children. *Environ. Res.* 147, 32–43.
- Nordby, K.C., Andersen, A., Irgens, L.M., Kristensen, P., 2005. Indicators of mancozeb exposure in relation to thyroid cancer and neural tube defects in farmers' families. *Scand. J. Work. Environ. Health* 31 (2), 89–96.
- Nueda, M.J., Martorell-Marugan, J., Martí, C., Tarazona, S., Conesa, A., 2018. Identification and visualization of differential isoform expression in RNA-seq time series. *Bioinforma. (Oxf., Engl.)* 34 (3), 524–526.
- Okazaki, K., Anzawa, H., Liu, Z., Ota, N., Kitamura, H., Onodera, Y., Alam, M.M., Matsumaru, D., Suzuki, T., Katsuka, F., Tadaka, S., Motoike, I., Watanabe, M., Hayasaka, K., Sakurada, A., Okada, Y., Yamamoto, M., Suzuki, T., Kinoshita, K., Sekine, H., Motohashi, H., 2020. Enhancer remodeling promotes tumor-initiating activity in NRF2-activated non-small cell lung cancers. *Nat. Commun.* 11 (1), 5911.
- Paganotto Leandro, L., Siqueira, D.E., Mello, R., Da Costa-Silva, D.G., et al., 2021. Behavioral changes occur earlier than redox alterations in developing zebrafish exposed to Mancozeb. In: Environmental pollution (Barking, Essex: 1987), 268, 115783.
- Palzes, V.A., Sagiv, S.K., Baker, J.M., Rojas-Valverde, D., Gutierrez-Vargas, R., Winkler, M.S., Fuhrmann, S., Staudacher, P., Menezes-Filho, J.A., Reiss, A.L., Eskenazi, B., Mora, A.M., 2019. Manganese exposure and working memory-related brain activity in smallholder farmworkers in Costa Rica: Results from a pilot study. *Environ. Res.* 173, 539–548.
- Pardali, E., Sanchez-Duffhues, G., Gomez-Puerto, M.C., Ten Dijke, P., 2017. TGF-β-induced endothelial-mesenchymal transition in fibrotic diseases. *Int. J. Mol. Sci.* 18 (10), 2157.
- Pariseau, J., McKenna, P., Aboelkhair, M., Saint-Louis, R., Pelletier, É., Davidson, T.J., Tremblay, R., Berthe, F.C.J., Siah, A., 2011. Effects of pesticide compounds (chlorothalonil and mancozeb) and benzo[a]pyrene mixture on aryl hydrocarbon receptor, p53 and ubiquitin gene expression levels in haemocytes of soft-shell clams (*Mya arenaria*). *Ecotoxicol. (Lond., Engl.)* 20 (8), 1765–1772.
- Patel, J., Bircan, E., Tang, X., Orloff, M., Hobbs, C.A., Browne, M.L., Botto, L.D., Finnell, R.H., Jenkins, M.M., Olshan, A., Romitti, P.A., Shaw, G.M., Werler, M.M., Li, J., Nemphard, W.N., National Birth Defects Prevention, S., 2021. Paternal genetic variants and risk of obstructive heart defects: a parent-of-origin approach. *PLoS Genet.* 17 (3), 1009413.
- Peng, X., Fan, S., Tan, J., Zeng, Z., Su, M., Zhang, Y., Yang, M., Xia, L., Fan, X., Cai, W., Tang, W.H., 2020. Wnt2bb induces cardiomyocyte proliferation in zebrafish hearts via the jnk1/c-jun/creb1 pathway. *Front. Cell Dev. Biol.* 8, 323.
- Phng, L.K., Potente, M., Leslie, J.D., Babbage, J., Nyqvist, D., Lovob, I., Ondr, J.K., Rao, S., Lang, R.A., Thurston, G., Gerhardt, H., 2009. Nrarp coordinates endothelial Notch and Wnt signaling to control vessel density in angiogenesis [J]. *Dev. Cell* 16 (1), 70–82.
- Qiu, W., Chen, B., Greer, J.B., Magnuson, J.T., Xiong, Y., Zhong, H., Andrzejczyk, N.E., Zheng, C., Schlenk, D., 2020. Transcriptomic responses of bisphenol s predict involvement of immune function in the cardiotoxicity of early life-stage zebrafish (*Danio rerio*). *Environ. Sci. Technol.* 54 (5), 2869–2877.
- Rahman, S.M., Kippler, M., Tofail, F., Bölte, S., Hamadani, J.D., Vahter, M., 2017. Manganese in drinking water and cognitive abilities and behavior at 10 Years of age: a prospective cohort study. *Environ. Health Perspect.* 125 (5), 057003.

- Rao, Y., Wan, Q., Su, H., Xiao, X., Liao, Z., Ji, J., Yang, C., Lin, L., Su, J., 2018. ROS-induced HSP70 promotes cytoplasmic translocation of high-mobility group box 1b and stimulates antiviral autophagy in grass carp kidney cells [J]. *J. Biol. Chem.* 293 (45), 17387–17401.
- Del Re, D.P., Amgalan, D., Linkermann, A., Liu, Q., Kitsis, R.N., 2019. Fundamental mechanisms of regulated cell death and implications for heart disease. *Physiol. Rev.* 99 (4), 1765–1817.
- Robinson, M.D., McCarthy, D.J., Smyth, G.K., 2010. edgeR: a bioconductor package for differential expression analysis of digital gene expression data. *Bioinforma. (Oxf., Engl.)* 26 (1), 139–140.
- Runkle, J., Flocks, J., Economos, J., Dunlop, A.L., 2017. A systematic review of Mancozeb as a reproductive and developmental hazard. *Environ. Int.* 99, 29–42.
- Salamanca-Fernández, E., Rodríguez-Barranco, M., Petrova, D., Larrañaga, N., Guevara, M., Moreno-Iribas, C., Chirlaque, M.D., Colorado-Yohar, S., Arrebola, J.P., Vela, F., Olea, N., Agudo, A., Sánchez, M.J., 2020. Bisphenol A exposure and risk of ischemic heart disease in the spanish european prospective investigation into cancer and nutrition study. *Chemosphere* 261, 127697.
- Salguero-Jiménez, A., Grego-Bessa, J., D'amato, G., Jiménez-Borreguero, L.J., de la Pompa, J.L., 2018. Myocardial Notch1-Rbpj deletion does not affect NOTCH signaling, heart development or function. *PLoS One* 13 (12), 0203100.
- Sarmah, S., Marrs, J.A., 2016. Zebrafish as a vertebrate model system to evaluate effects of environmental toxicants on cardiac development and function. *Int. J. Mol. Sci.* 17 (12), 2123.
- Shankar, P., Dasgupta, S., Hahn, M.E., Tanguay, R.L., 2020. A review of the functional roles of the zebrafish Aryl hydrocarbon receptors. *Toxicol. Sci.: Off. J. Soc. Toxicol.* 178 (2), 215–238.
- Song, Y.J., Zhong, C.B., Wang, X.B., 2019. Heat shock protein 70: a promising therapeutic target for myocardial ischemia-reperfusion injury. *J. Cell. Physiol.* 234 (2), 1190–1207.
- Stadler, S.C., Allis, C.D., 2012. Linking epithelial-to-mesenchymal-transition and epigenetic modifications. *Semin. Cancer Biol.* 22 (5–6), 404–410.
- Stephenson, O.J., Trombetta, L.D., 2020. Comparative effects of Mancozeb and disulfiram-induced striated muscle myopathies in long-evans rats. *Environ. Toxicol. Pharmacol.* 74, 103300.
- Tanaka, K., Kato, A., Angelocci, C., Watanabe, M., Kato, Y., 2014. A potential molecular pathogenesis of cardiac/laterality defects in Oculo-Facio-Cardio-Dental syndrome. *Dev. Biol.* 387 (1), 28–36.
- Tanner, J.P., Salemi, J.L., Stuart, A.L., Yu, H., Jordan, M.M., DuClos, C., Cavicchia, P., Correia, J.A., Watkins, S.M., Kirby, R.S., 2015. Associations between exposure to ambient benzene and PM(2.5) during pregnancy and the risk of selected birth defects in offspring. *Environ. Res.* 142, 345–353.
- Tian, W., Guo, H.S., Li, C.Y., Cao, W., Wang, X.Y., Mo, D., Hao, X.W., Feng, Y.D., Sun, Y., Lei, F., Zhang, H.N., Zhao, M.G., Li, X.Q., 2019. PFKFB3 promotes endotoxemia-induced myocardial dysfunction through inflammatory signaling and apoptotic induction. *Toxicol. Appl. Pharmacol.* 368, 26–36.
- Tilton, F., La Du, J.K., Vue, M., Alzarban, N., Tanguay, R.L., 2006. Dithiocarbamates have a common toxic effect on zebrafish body axis formation. *Toxicol. Appl. Pharmacol.* 216 (1), 55–68.
- Toydemir, G., Loonen, L., Venkatasubramanian, P.B., Mes, J.J., Wells, J.M., De Wit, N., 2021. Coffee induces AHR- and Nrf2-mediated transcription in intestinal epithelial cells. *Food Chem.* 341 (Pt 2), 128261.
- Wang, Z., Kottawatta, K., Kodithuwakku, S.P., Fernando, T.S., Lee, Y.L., Ng, E., Yeung, W., Lee, K.F., 2021. The fungicide Mancozeb reduces spheroid attachment onto endometrial epithelial cells through downregulation of estrogen receptor β and integrin $\beta 3$ in Ishikawa cells. *Ecotoxicol. Environ. Saf.* 208, 111606.
- Van Wendel De Joode, B., Barbeau, B., Bouchard, M.F., et al., 2016. Manganese concentrations in drinking water from villages near banana plantations with aerial mancozeb spraying in Costa Rica: results from the Infants' Environmental Health Study (ISA) [J]. In: Environmental pollution (Barking, Essex: 1987), 215, pp. 247–257.
- Van Wendel De Joode, B., Mora, A.M., Córdoba, L., Cano, J.C., Quesada, R., Faniband, M., Wesseling, C., Ruepert, C., Oberg, M., Eskenazi, B., Mergler, D., Lindh, C.H., 2014. Aerial application of mancozeb and urinary ethylene thiourea (ETU) concentrations among pregnant women in Costa Rica: the Infants' Environmental Health Study (ISA). *Environ. Health Perspect.* 122 (12), 1321–1328.
- Zeng, C., Xing, R., Liu, J., Xing, F., 2016. Role of CSL-dependent and independent Notch signaling pathways in cell apoptosis. *Apoptosis: Int. J. Program. Cell Death* 21 (1), 1–12.
- Zhai, C., Lv, J., Wang, K., Li, Q., Qu, Y., 2019. HSP70 silencing aggravates apoptosis induced by hypoxia/reoxygenation in vitro. *Exp. Ther. Med.* 18 (2), 1013–1020.
- Zhang, M., Wang, C., Hu, J., Lin, J., Zhao, Z., Shen, M., Gao, H., Li, N., Liu, M., Zheng, P., Qiu, C., Gao, E., Wang, H., Sun, D., 2015. Notch3/Akt signaling contributes to OSM-induced protection against cardiac ischemia/reperfusion injury. *Apoptosis: Int. J. Program. Cell Death* 20 (9), 1150–1163.
- Zheng, Y., Kong, J., Li, Q., Wang, Y., Li, J., 2018. Role of miRNAs in skeletal muscle aging. *Clin. Interv. Aging* 13, 2407–2419.